

**M. Jażdżewska**

*Gdansk University of Technology, Department of Materials Engineering and Welding,  
Narutowicza 11/12, 80-233 Gdansk, Poland  
magdalena.jazdzewska@pg.edu.pl*

## **EFFECTS OF CO<sub>2</sub> AND Nd:YAG LASER REMELTING OF THE Ti6Al4V ALLOY ON THE SURFACE QUALITY AND RESIDUAL STRESSES**

### ABSTRACT

The titanium alloys are materials susceptible to tribological wear and the laser treatment can be applied in surface treatment processes to obtain for example higher hardness level. From the other side, it is important to take into consideration, that hardness increase that can be connected with cracks. The aim of this research was to investigate the effects of different lasers and the process parameters on the form and level of residual stresses in the Ti6Al4V alloy, which determine the initiation and propagation of cracking. Two lasers were used, the CO<sub>2</sub> and Nd:YAG lasers. The specimens were remelted in liquid nitrogen, water or calm air at different pre-heating temperature. The different laser power and scan rates were applied. The increase in energy density increased the number of cracks, the change of an environment and pre-heating affected also the surface cracking. The cracks observed after remelting with Nd:YAG laser were longer than those observed after treatment with CO<sub>2</sub> laser. The compressive stresses after the CO<sub>2</sub> laser treatment, and tensile stresses after treatment with the Nd:YAG laser, were found. The appearance of cracks was attributed to an excessive energy density. The different distribution of heat energy inside and around the laser tracks was discussed as the origin of presence either tensile or compressive stresses in the alloy treated with different lasers.

**Keywords:** *Ti alloys; laser treatment; residual stresses*

### INTRODUCTION

The various surface modification technologies of titanium and its alloys have been applied to improve their properties. Among such techniques, the laser treatment has become one of the more promising alternatives. The methods of laser processing include the solid state hardening, melting, alloying, cladding, ablation, shot peening, cleaning, texturing and welding [1-4]. The microstructure modification include grain refinement and formation of supersaturated solid solutions, and fine dispersions of particles, causing the hardening and strengthening of the surface layer. The resistance to wear, corrosion, erosion, high temperature, and biocompatibility are dependent on laser processing parameters, which influence the microstructure, in particular formation of oversaturated solid solutions and an appearance of high compressive stresses [5-9].

As concerns titanium and its alloys, the laser melting has been performed relatively seldom. In one attempt [4], the low power laser was applied to create the surface porosity of different magnitude. The modified surface demonstrated the significant increase of osseointegration. In tests made with the short pulse Cr-F UV laser on the Ti-6Al-4V and Ti-6.8Mo-4.5Fe-1.5Al alloys [10-12] the relatively smooth, crack-free nanocrystalline surface layers were obtained containing significant amounts of martensite. The laser melting of pure titanium with the Nd:YAG laser showed no pitting corrosion as compared to no-melted alloy, likely because of microstructural changes caused by rapid solidification after laser remelting [13]. For the AlSi12CuNiMg alloy after solidification of surface remelted layer, a fine-grained microstructure was formed at a depth of 270-420  $\mu\text{m}$ , and a significant increase in microhardness was observed [14]. The new WaveShape approach, based on a sinusoidal modulation of laser power was said to be especially suitable for the Ti-Al6-4V alloy [15].

The residual stresses results from elastoplastic deformations induced in the workpiece material during the heat treatment process, their extent and magnitude depending on temperature conditions in heating and cooling, and physical properties of the material. Such stresses are induced by both temperature difference and microstructural change between the surface and the core of the specimen [16,17]. The residual stresses distribution can be optimized by using for example numerical simulation as a modern method of prediction and optimization [17-20]. The occurrence of residual stresses after laser treatment was observed for zirconium [18], nodular cast iron [21], work tool steel [22], quality construction steel [23], and titanium [24].

The presence of compressive residual stresses is very desired as they increase the fatigue strength of the material [21]. The effect appears within the thin surface zone. The compressive strains were observed in a steel reaching 150 MPa value [23]. The residual stresses tended to change from tensile to compressive ones with increasing number of laser beads due to pre-heating effect [22]. Contraction of remelted zone during cooling after laser treatment produced tensile stresses responsible for cracking of brittle materials [25]. The precipitation annealing caused an almost complete disappearance of tensile residual stresses at the surface of the remelted layer [14].

So far research has shown that the laser treatment may result in an appearance of compressive stresses up to some depth together with an occurrence of the melted zone. The possibility to make melting of non-ferrous alloys, namely Al, Cu and Ti ones, in cryogenic conditions, i.e., in liquid nitrogen, was proposed to obtain the critically fast quenching [26-28]. However, for the last material, the presence of cracks was observed. This research was aimed to investigate, by what manner the laser treatment parameters, like laser type, laser power, scan rate and other factors affect the tendency to crack, and whether the magnitude and sign of residual stresses may be taken into account to explain the observed effects.

## MATERIALS AND METHODS

The specimens were made of the Ti6Al4V alloy (Fe 0.16, V 4.05, Al 6.40, C 0.01, N 0.005 wt.pct.) Grade 5 manufactured by TIMET Company from United Kingdom. The 12 mm thick sheets were delivered as hot rolled, annealed at 750°C, with removed mill scale and etched.

The laser remelting with the CO<sub>2</sub> TRUMPF TLF 6000 Turbo was performed at the Center for Laser Technologies, Kielce University of Technology. The rectangular laser beam



of 1x20 mm dimensions was applied at 10 mm distance between the laser head and specimen surface. Before treatment, the specimens were cleaned with acetone and covered with an absorbing substance with graphite as a main component. Each specimen was remelted in one passage of the laser. The treatment was performed in liquid nitrogen; specimens were immersed about 1 mm below the coolant surface, at -195°C temperature. Some specimens were pre-heated to some elevated temperatures (200 – 550°C) and before remelting. The parameters of cryogenic laser remelting are shown in Table 1.

The laser remelting with the Nd:YAG laser was carried out also at the Kielce University of Technology. Before laser remelting the specimens were cleaned with acetone. The laser treatment was made in calm air at room temperature at a pulse frequency 50 Hz and 50% overlapping laser beams, and was carried out in argon atmosphere. The laser treatment parameters are shown in Table 2.

**Table 1.** Laser treatment parameters of the Ti6Al4V alloy by CO<sub>2</sub> laser in cryogenic conditions

Power [W]	Beam dimensions [mm]	Scan rate [m/min]	Power density [W/cm <sup>2</sup> ]	Energy density [Ws/cm <sup>2</sup> ]
3000	1x20	1.0	15000	900
4000	1x20	1.0	20000	12000
5000	1x20	1.0	25000	15000
6000	1x20	1.0	30000	18000
5000	1x20	0.5	25000	30000
6000	1x20	0.5	30000	36000

**Table 2.** Laser treatment parameters of the titanium alloy Ti6Al4V by Nd:YAG laser

Power [W]	Beam dimensions [mm]	Scan rate [m/min]	Power density [W/cm <sup>2</sup> ]	Energy density [Ws/cm <sup>2</sup> ]
150	φ 1.0	0.25	4777	446
150	φ 1.0	0.50	4777	225
150	φ 1.0	1.00	4777	112
150	φ 1.0	1.50	4777	75
150	φ 1.0	2.00	4777	56
150	φ 1.0	4.00	4777	19

The microscopic examinations of the surface layer of the remelted alloy were made with the Philips XL – 30 SEM. The observations were performed on cross-sections perpendicular to the laser beam direction. The metallographic sections were prepared by grinding with abrasive papers, No. 1200 paper as the last, followed by the polishing with alumina-water suspension and diamond pastes, and etching with the Kroll reagent (0.06 mm<sup>3</sup> HF, 0.12 mm<sup>3</sup> HNO<sub>3</sub> and distilled water to a volume of 50 mm<sup>3</sup>). The crack depths were assessed using the Multiscan software.

The phase analysis and measurement of residual stresses were carried out with the Philips PW 1710 X-ray diffractometer equipped with the ATC-3 texture goniometer at the Institute of Materials Engineering and Metallurgy, Polish Academy of Sciences, in Krakow. To measure the stresses, the indirect method  $\sin^2\theta$  was applied, based on examinations of shift of

diffraction lines in the stressed crystalline material. The measurements were made on flat specimen surfaces.

## RESULTS

The examples of the surface topography of remelted specimens are shown in Figs. 1 and 2. For the CO<sub>2</sub> laser, discontinuity of remelted zone, waviness patterning the laser passages and transcrystalline cracking forming a network are visible. At varied laser work parameters, for both continuous work CO<sub>2</sub> laser and Nd:YAG short pulse laser, the cracks appeared always inside the remelted zone of the Ti6Al4V alloy. The cracks observed after treatment with Nd:YAG laser run across an entire remelted zone, up to 5 μm from the surface. Additionally, after remelting with the CO<sub>2</sub> laser of pre-heated specimens, the blisters appeared up to 50 μm from the surface.

The grain refinement was observed with the SEM after laser remelting. The thickness of remelted zone was determined by laser treatment parameters. The thickest layers, about 450 μm, were achieved after remelting with a CO<sub>2</sub> laser at 6000 W laser power and 0.5 m/min scan rate. For pre-heated specimens, the average thickness of remelted zone achieved 200 μm; no effect of pre-heating temperature on the layer thickness was observed. For Nd:YAG laser, the thickness of remelted layer was about 5 μm.

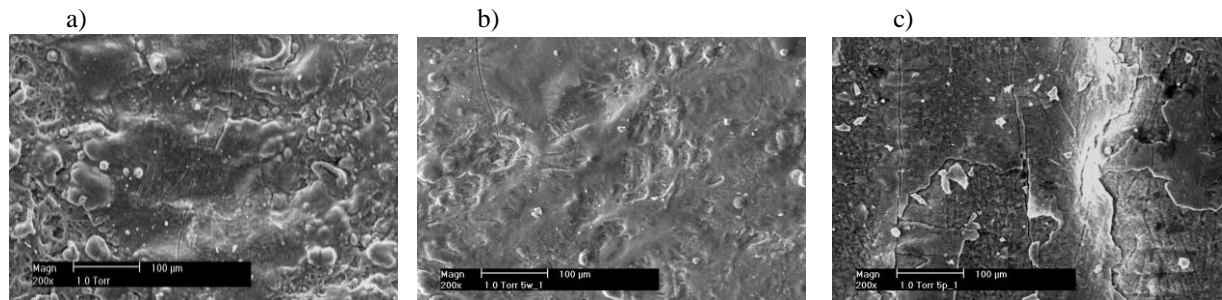


**Fig. 1.** Surface topography microstructure of the Ti6Al4V alloy after CO<sub>2</sub> laser treatment in: a) liquid nitrogen, b) tap water, c) calm air (5000 W, 1 m/min)

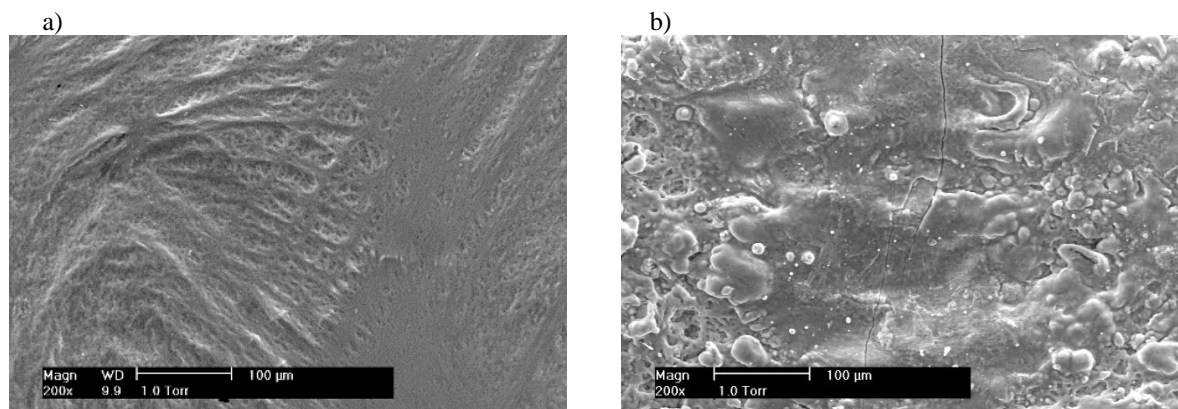


**Fig. 2.** Surface microstructure of the Ti6Al4V alloy after a) Nd:YAG laser remelting (150 W, 1 m/min), b) preheated in 500°C CO<sub>2</sub> laser remelting (5000 W, 1 m/min)

The assessment of crack density (amount of crack on the surface area), maximum and average crack depth for CO<sub>2</sub> laser treated specimens is listed in Table 3. Neither laser treatment parameters nor environment affected the observed effects to significant degree. It is to note that the cracks in CO<sub>2</sub> laser treated alloy grew to about 20-40% of the thickness of remelted layer, and for Nd:YAG laser, the cracks penetrated across the whole layer (Fig. 3).

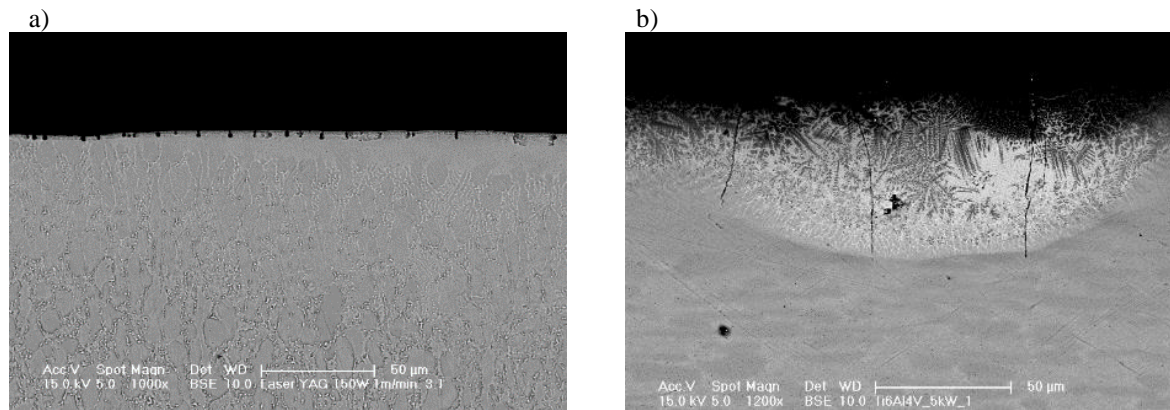


**Fig. 3.** The cross section of the Ti6Al4V alloy after a) Nd:YAG laser remelting (150 W, 1 m/min), b) preheated in 500°C CO<sub>2</sub> laser remelting (5000 W, 1 m/min)

**Table 3.** Number and depth of cracks in the Ti6Al4V alloy surface laser melted in different conditions

Laser treatment parameters	Thickness of remelted layer [µm]	Number of cracks [µm <sup>-2</sup> ]	Depth of cracks [µm]	
			maximum	average
3 kW, 1 m/min, LN	248	0.31	40	21
4 kW, 1 m/min, LN	298	0.82	43	26
5 kW, 1 m/min, LN	357	0.22	45	28
6 kW, 1 m/min, LN	264	0.81	37	28
5 kW, 0.5 m/min, LN	473	0.43	55	43
6 kW, 0.5 m/min, LN	454	1.09	36	29
5 kW, 1 m/min, air	140	1.41	37	30
5 kW, 0.25 m/min, air	240	0.08	94	47
5 kW, 1 m/min, water	140	1.80	62	30
5 kW, 0.25 m/min, water	240	0.99	106	47
5 kW, 1 m/min, 200°C, air	184	0.18	65	30
5 kW, 1 m/min, 300°C, air	199	0.48	72	22
5 kW, 1 m/min, 400°C, air	205	0.21	84	55
5 kW, 1 m/min, 450°C, air	180	0.34	43	24
5 kW, 1 m/min, 500°C, air	196	0.19	34	24
5 kW, 1 m/min, 550°C, air	172	0.15	82	33

The residual stresses have different values and sign, depending on remelting conditions. Fig. 4 shows the results of calculations for specimens remelted with a CO<sub>2</sub> laser at 5000 and 6000 W laser power, at 1 m/min scan rate, treated in liquid nitrogen, water, and air, and those remelted with Nd:YAG laser at 150 W laser power and 1 m/min. scan rate. The highest was the stress after remelting in liquid nitrogen at 5000 W laser power and 1 m/min. scan rate, namely 1796 MPa. It is much more than any other so far reported value. Only compressive stresses (negative sign) appeared for CO<sub>2</sub> laser and only tensile stresses for the Nd:YAG laser.





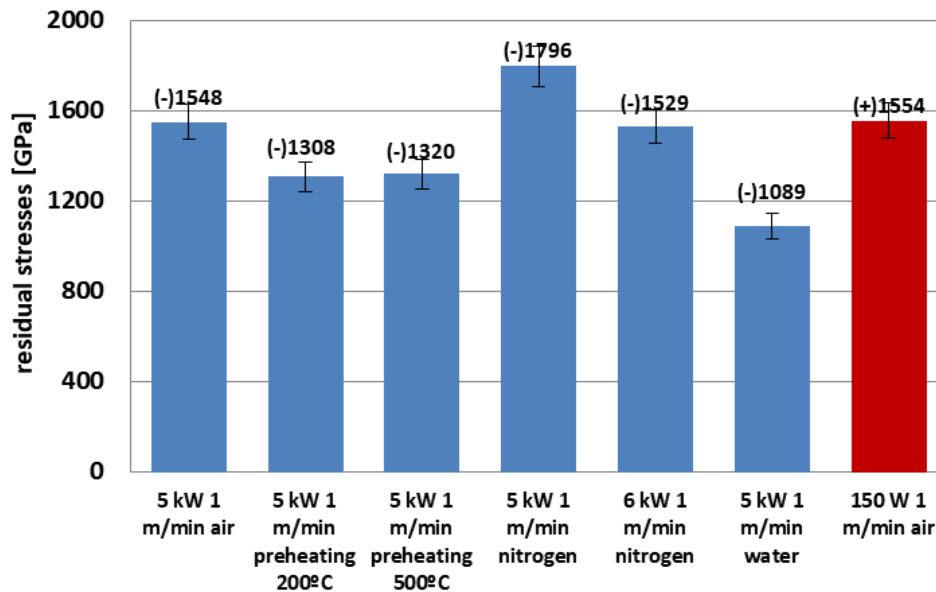


Fig. 4. Residual stresses in the surface layers of the Ti6Al4V alloy obtained after laser remelting with different parameters

## DISCUSSION

The compressive residual stresses may influence the material properties and its lifetime in real conditions. The CO<sub>2</sub> laser surface remelting results, as demonstrated here, in high compressive residual stresses. Surprisingly, a use of the Nd:YAG laser causes an appearance of high tensile residual stresses, 1554 MPa. Presumably for that reason, the cracks after CO<sub>2</sub> laser treatment are limited to some depth value, but after Nd:YAG laser treatment they run across the whole layer.

It is not easy to explain why the residual stresses have opposite signs for different lasers, and why the cracks are always observed, even for alloy pre-heated and melted in water or air, contrary to some earlier reports. Probably, could be helpful to use numerical simulation to explain phenomena of tensile and compressive stresses creation in the treated specimens. The front between the liquid and solid phases propagates inside the material as the heat is conducted from the surface into the material bulk, and the surface temperature increases until heat conduction and the heats of melting and evaporation balance the surface energy deposition. The melting of the substrate occurs rapidly only at the surface, while the bulk of the material remains cool, thus serving as an infinite heat sink [4]. Titanium and its alloys have relatively low conductivity, comparing to copper and aluminum alloys so that the heat after laser energy absorption is not fast enough transmitted into the bulk. Also, the martensitic transformation in the Ti6Al4V alloy enhances an initiation of cracks. The appearance or a lack of cracks, in other investigations, is strictly related to the laser energy. The cracks are formed when the absorbed energy is too high, the created heat energy is also too high to be quickly dispersed into the bulk, the difference in temperature of surface and a bulk results in high stresses, and simultaneously the martensitic transformation brings out the additional residual stresses.

## CONCLUSIONS

The laser treatment conditions affect the number and length of cracks. The increase in laser power increases the number of cracks, the change of an environment from liquid nitrogen to calm air and water increase both the number and depth of cracks, the pre-heating of specimens results in the decrease in the number of cracks, and the cracks observed after remelting with Nd:YAG laser are longer than those observed after treatment with CO<sub>2</sub> laser.

The residual stresses are the highest for specimens cooled in liquid nitrogen, in this case the thickest melted layer is also observed. The compressive stresses after this treatment, and tensile stresses after treatment with Nd:YAG laser, are found.

The appearance of cracks may be attributed to an excessive energy density for CO<sub>2</sub> laser. The different distribution of heat energy inside and around the laser tracks may explain the presence either tensile or compressive stresses after the treatment of the Ti6Al4V alloy with the Nd:YAG and CO<sub>2</sub> laser, respectively.

## ACKNOWLEDGMENTS

The author thanks Prof. Andrzej Dziadoń for their technical assistance in some tests. The helpful comments of Prof. Andrzej Zielinski are gratefully acknowledged.

## REFERENCES

1. Kusiński J., Kac S., Kopia A., Radziszewska A., Rozmus-Górnikowska M., Major B., Major L., Marczak J., Lisiecki A.: Laser modification of the materials surface layer – a review paper. *Bulletin of the Polish Academy Of Sciences, Technical Sciences*, 4 (2012) 711-728.
2. Candel J. J., Amigó V.: Recent advances in laser surface treatment of titanium alloys. *Journal of Laser Applications*, 23 (2011) 1-7.
3. Quazi, M. M., Ishak, M., Fazal, M. A., Arslan, A., Rubaiee, S., Aiman, M. H., Sultan T., Manladan, S. M.: A comprehensive assessment of laser welding of biomedical devices and implant materials: recent research, development and applications. *Critical Reviews in Solid State and Materials Sciences*, (2020) 1-43.
4. Götz H.,E., Müller M. Emmel A., Holzwarth U., Erben R.G., Stangl R.: Effect of surface finish on the osteointegration of laser-treated titanium alloy implants. *Biomaterials* 25 (2004) 4057-4064.
5. Tęczar P., Majkowska-Marzec B., Bartmański M.: The influence of laser alloying of Ti13Nb13Zr on surface topography and properties. *Advances in Materials Science*, 19 (2019) 44-56.
6. Majkowska-Marzec, B., Rogala-Wielgus, D., Bartmański, M., Bartosewicz, B., Zieliński, A.: Comparison of properties of the hybrid and bilayer MWCNTs—hydroxyapatite coatings on Ti alloy. *Coatings*, 9 (2019) 643.
7. Landowski, M.: Influence of parameters of laser beam welding on structure of 2205 duplex stainless steel. *Advances in Materials Science*, 19 (2019) 21-31.



8. Zeng, C., Wen, H., Etefagh, A. H., Zhang, B., Gao, J., Haghshenas, A., Raush J.R. Guo, S. M. (2020). Laser nitriding of titanium surfaces for biomedical applications. *Surface and Coatings Technology*, 385 (2020) 125397.
9. Lisiecki, A.: Study of optical properties of surface layers produced by laser surface melting and laser surface nitriding of titanium alloy. *Materials*, 12 (2019) 3112
10. Yue T.M., Cheung T.M., Man H.C.: The effects of laser surface treatment on the corrosion properties of Ti-6Al-4V alloy in Hank's solution. *Journal Materials Science Letters*, 19 (2000) 205-208.
11. Yue T.M., Yu J.K., Mei Z., Man H.C.: Excimer laser surface treatment of Ti-6Al-4V alloy for corrosion resistance enhancement. *Materials Letters*, 52 (2002) 206-212.
12. Guillemot F., Prima E., Tokarev V.N., Belin C., Porté-Durrieu M.C., Gloriant T., Baquey Ch., Lazare S.: Ultraviolet laser surface treatment fore biomedical applications of  $\beta$  titanium alloys: morphological and structural characterization. *Applied Physics A*, 77 (2003) 899-904.
13. Sun Z., Annergren I., Pan D., Mai T.A.: Effect of laser surface remelting on the corrosion behavior of commercially pure titanium sheet. *Materials Science and Engineering: A*, 345 (2003) 293-300.
14. Sušnik J., Sturm R., Grum J.: Influence of laser surface remelting on Al-Si alloy properties. *Journal of Mechanical Engineering*, 58 (2012) 614-620.
15. Temmler A., Walochnik M. A., Willenborg E., Wissenbach K.: Surface structuring by remelting of titanium alloy Ti6Al4V. *Journal of Laser Applications*, 27 (2015) 29103.
16. Grum J., Šturm R.: Residual stress state after the laser surface remelting process. *Journal of Materials Engineering and Performance*, 10 (2001) 270.
17. Šturm R., Grum J.: Influence of laser remelting process on strain and residual stresses in nodular iron. *Materials Science Forum*, 681 (2011) 188-193
18. Yilbas B. S., Akhtar S. S., Matthews A., Karatas C.: Laser remelting of zirconia surface: investigation into stress field and microstructures. *Materials and Manufacturing Processes*, 26 (2011) 1277-1287.
19. Kik, T., & Górká, J.: Numerical simulations of laser and hybrid S700MC T-joint welding. *Materials*, 12(3) (2019) 516.
20. Kik, T.: Computational techniques in numerical simulations of arc and laser welding processes. *Materials*, 13(3) (2020) 608.
21. Grum J., Šturm R.: Influence of laser remelting process parameters on residual stresses in nodular cast iron. *Materials and Manufacturing Processes*, 15 (2000) 815-827.
22. Preußner J., Oeser S., Pfeiffer W., Temmler A., Willenborg E.: Microstructure and residual stresses of laser remelted surfaces of a hot work tool steel. *International Journal of Materials Research*, 105 (2014) 328-336.
23. Bylica A., Bochnowski W., Więcek G.: Residual stresses in the laser remelted C45 steel. *Archiwum Odlewnictwa*, 6 (2006) 43-48 (in Polish).
24. Gusarov A.V., Pavlov M., Smurov I.: Residual stresses at laser surface remelting and additive manufacturing. *Physics Procedia*, 12 (2011) 248–254.
25. Majkowska B., Serbiński W.: Analysis of residual stresses in laser remelted surface layer of the SUPERSTON alloy for ship propellers. *Inżynieria Materiałowa* 6 (2009) 501-504 (in Polish).
26. Serbiński W., Olive J. M., Rudnicki J.: Laser surface treatment of aluminium-silicon alloy at cryogenic conditions. *Advances in Materials Science*, 3 (2003) 51-59



27. Majkowska B., Serbiński W.: Microstructure and corrosion properties of the laser treated SUPERSTON alloy. *Journal of Achievements in Materials and Manufacturing Engineering*, 18 (2006) 415-418.
28. Zieliński A., Jazdzewska M., Łubiński J., Serbiński W.: Effects of laser remelting at cryogenic conditions on microstructure and wear resistance of the Ti6Al4V alloy applied in medicine. *Solid State Phenomena*, 183 (2012) 215-224.